

Neutrino Oscillations in Intermediate States II

— *Wave Packets* —

Akinori Asahara¹, Kenzo Ishikawa¹, Takashi Shimomura¹
and Tetsuo Yabuki²

(1) *Department of Physics, Faculty of Science, Hokkaido University*
Sapporo 060-0810, Japan

(2) *Rakuno Gakuen University, Ebetsu 069-0836, Japan*

Abstract

We analyze oscillations of intermediate neutrinos in terms of the scattering of particles described by Gaussian wave packets. We study a scalar model as in a previous paper (I) but in realistic situations, where the two particles of the initial state and final state are wave packets and neutrinos are in the intermediate state. The oscillation of the intermediate neutrino is found from the time evolution of the total transition probability between the initial state and final state. The effect of a finite lifetime and a finite relaxation time are also studied. We find that the oscillation pattern depends on the magnitude of wave packet sizes of particles in the initial state and final state and the lifetime of the initial particle. For $\Delta m_{21}^2 = 3 \times 10^{-2} \text{ eV}^2$, the oscillation probability deviates from that of the standard formula if the wave packet sizes are around 10^{-13} m for 0.4 MeV neutrino.

§1. Introduction

Neutrino oscillation is the only phenomenon in which to see effects of neutrino masses at present. To analyze neutrino oscillations, single particle wave functions have mainly been studied. Because neutrino masses are very important, it is necessary to understand the quantum mechanics of neutrino oscillations in full detail. It is the purpose of the present paper to study quantum mechanical aspects of neutrino oscillations beyond the single particle picture. We studied particle oscillations from a nonstandard viewpoint in the framework of quantum field theory, where neutrinos are in the intermediate state and the finite time interval effect is explicitly taken into account, on the basis of plane waves in a previous paper.¹⁾ We found that non-standard oscillation patterns emerge in the exact plane waves. In many real physical processes, however, particles are not exact plane waves but have finite spatial extensions. Wave packets are suitable to express these particles. We study particle oscillations in terms of the scattering amplitude of the particles described by Gaussian wave packets. Neutrinos are in the intermediate state in this amplitude, and neutrino oscillation is studied from this amplitude.

In scattering processes, the roles and importance of wave packets have been stressed by Goldberger and Watson.²⁾ The size of the wave packet of the initial state is determined from the beam size, and it is a semi-micro scale for hadron beams. This corresponds to an energy scale of the order of eV or less. By contrast, typical energy scales of hadron systems are of the order of a few hundred MeV. Hence the effects of wave packets in the initial state are negligible in standard hadron experiments. The size of the wave packet of the final state, on the other hand, is determined by a detector. A detector is composed of many systems of materials. We regard the minimum set of materials for which a classical signal is taken as a unit detector. A unit detector is composed of atoms and generates radiation, electrons, or other particles by which information from the quantum wave function is transmitted to classical observers. The wave packet size is determined from the unit detector and the resolution of the measurement is also determined from the unit detector. Hence the wave packet size should be about the same as the spatial resolution of the detector. A unique value of this size is not known now, so we study the dependence of the transition probability on the wave packet sizes. The time resolution is determined from the time evolution of the detector. In this paper, for simplicity, it is assumed that the time resolution is zero. Two observations at different times are assumed to be independent.

In neutrino oscillation experiments, the typical energy scale is extremely small and the spatial sizes of experiments are of the order several hundreds km or more and are very different from scales of ordinary experiments. Hence, the roles of wave packets in neutrino

experiments are different from their roles in other ordinary experiments and they should be clarified. It is one of our purposes in the present work to study these problems. In fact, several theoretical works have been done on Gaussian wave packets. But they are not sufficient. Especially, qualitative analysis is lacking. We study effects that have not been studied to this time. The works in Refs. 3)–5) treat neutrinos as wave packets in a single particle picture. Other works treat the particles in the initial and final states as wave packets in a field theoretical treatment.^{6),7)} In the latter, the standard S matrix theory, in which the transition time interval is set to infinity from the beginning, was used, and the dependence of the amplitudes on neutrino parameters was obtained. However, this standard treatment of the S matrix is inadequate in a process in which the finite time interval effect is important and the dependence of amplitudes on external particles' parameters are studied. The finite time interval effect becomes relevant in the situation in which the intermediate particle is very light and interacts weakly with matter. Especially when the intermediate particle consists of a superposition of several mass eigenstates and the mass squared difference is very small, the finite time interval effect is not negligible. In the standard S matrix theory, because the energy is strictly conserved and the interference of the amplitudes of different mass does not occur, there is no oscillation when all the particles are exact plane waves. In (I), the finite time interval effects in particle oscillations was shown to be important when the observed particles are exact plane waves. Thus the finite time interval effect should be important generally in the field theoretical treatment of neutrino oscillations. A modified S matrix approach that allows us to investigate finite time interval effects should be applied for the study of intermediate neutrino oscillations.

In the present paper, we extend our study of particle oscillations in the intermediate state to the wave packet formalism. Oscillation amplitudes of neutrinos in the intermediate state where the particles in the initial state and final state are described by wave packets are studied and effects due to the finite wave packet, the finite time interval, and the finite lifetime or finite relaxation time are found. Amplitudes are shown to deviate from the standard formula in extreme conditions, when the wave packet sizes are very small.

This paper is organized in the following manner. In Section 2 we give the general consideration of the wave packet formalism in which the particles in the initial and final states are described by Gaussian wave packets in the finite time interval method. In Section 3, the amplitude is computed using the Gaussian approximation. In Section 4, we include a finite lifetime and a finite relaxation time. In Section 5, numerical results in one spatial dimension are presented. A summary is given in Section 6.

§2. The wave packet formalism

Here we investigate neutrino oscillations in a scalar model in which particles in the initial and final states have finite spatial widths that are described by Gaussian wave packets. Particles A , B , C and D are external particles and are expressed by the field operators $\Phi_A(x)$, $\Phi_B(x)$, $\Phi_C(x)$ and $\Phi_D(x)$. The fields $\Phi_{I_1}(x)$ and $\Phi_{I_2}(x)$ are mass eigenstates and are internal particles. The Lagrangian density is given by

$$L = \sum_{L=A,B,C,D} \left(\frac{1}{2}(\partial_\mu \Phi_L)^2 - \frac{1}{2}m_L^2 \Phi_L^2 \right) + \sum_{i=1,2} \left(\frac{1}{2}(\partial_\mu \Phi_{I_i})^2 - \frac{1}{2}m_{I_i}^2 \Phi_{I_i}^2 \right) - H_{\text{int}}, \quad (2.1)$$

where m_{I_i} is the mass of Φ_{I_i} and m_L that of Φ_L . The interaction Hamiltonian is written

$$\begin{aligned} H_{\text{int}} &= H_{\text{int}}^1 + H_{\text{int}}^2, \\ H_{\text{int}}^1 &= F_1 \int d^3x \Phi_A(x) \Phi_{I_C}(x) \Phi_C(x), \\ H_{\text{int}}^2 &= F_2 \int d^3x \Phi_B(x) \Phi_{I_D}(x) \Phi_D(x), \end{aligned} \quad (2.2)$$

where F_1 and F_2 are coupling constants. The fields $\Phi_{I_C}(x)$ and $\Phi_{I_D}(x)$ in the above interaction Hamiltonian are linear combinations of the mass eigenstates :

$$\begin{aligned} \Phi_{I_C}(x) &= \cos \theta \cdot \Phi_{I_1}(x) + \sin \theta \cdot \Phi_{I_2}(x), \\ \Phi_{I_D}(x) &= -\sin \theta \cdot \Phi_{I_1}(x) + \cos \theta \cdot \Phi_{I_2}(x). \end{aligned} \quad (2.3)$$

Here θ is the mixing angle between Φ_{I_C} and Φ_{I_D} and between Φ_{I_1} and Φ_{I_2} .

Each field operator is expanded in the interaction representation as

$$\begin{aligned} \Phi_L(x) &= \int \frac{d^3p}{2E(p)_L} \exp\left(i\mathbf{p} \cdot \mathbf{x} - iE_L(p)t\right) \cdot a(\mathbf{p})_L + h.c., \\ E(\mathbf{p})_L &= \sqrt{\mathbf{p}^2 + m_L^2}, \end{aligned} \quad (2.4)$$

where L stands for A, B, C, D and I_i .

We investigate the situation in which the particles A and B are prepared at time $t = 0$ and position $\mathbf{x} = \mathbf{X}_A$, and the particles C and D are detected at $t = T_C$, $\mathbf{x} = \mathbf{X}_C$ and $t = T_D$, $\mathbf{x} = \mathbf{X}_D$, respectively. (Fig. 1) We assume $T_D > T_C$. The transition amplitude of the finite time interval T_D between the initial and final states at second order is calculated as

$$\langle \text{final} | S[t = T_D, t = 0] | \text{initial} \rangle = \langle \text{final} | i^2 \int_0^{T_D} dt_2 \int_0^{t_2} dt_1 H_{\text{int}}(t_1) H_{\text{int}}(t_2) | \text{initial} \rangle. \quad (2.5)$$

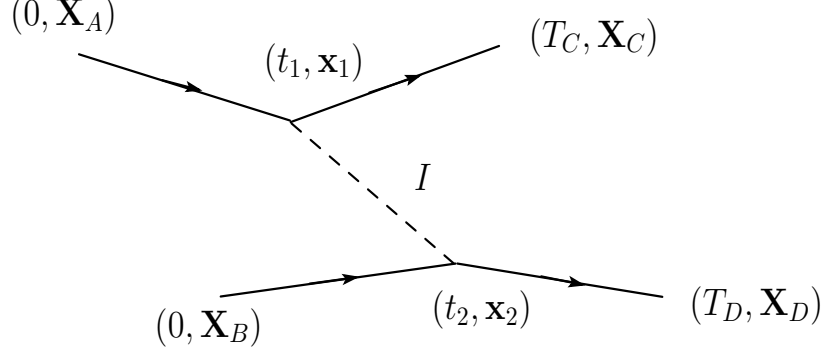


Fig. 1. Diagram

The initial state is composed of two particles, A and B , which are the wave packets of the finite spatial extents expressed by a distribution function. We assume that the initial time and the final time are defined with infinite precision. This assumption makes the wave packet states defined at different times independent of each other. The distribution function of the momentum \mathbf{p} , $w(\mathbf{p}; \mathbf{p}^0, \mathbf{X}, T; \sigma)$, has a finite extension around the central value \mathbf{p}^0 , and a Gaussian form of width σ is assumed :

$$w(\mathbf{p}; \mathbf{p}^0, \mathbf{X}, T; \sigma) = \exp \left(- \frac{(\mathbf{p} - \mathbf{p}^0)^2}{2\sigma^2} - i\mathbf{p} \cdot \mathbf{X} + iE(\mathbf{p})T \right). \quad (2.6)$$

The initial state is given by

$$\begin{aligned} |\text{initial}\rangle &= \int \frac{d^3 p_A}{\sqrt{(2\pi\sigma_A^2)^3}} \int \frac{d^3 p_B}{\sqrt{(2\pi\sigma_B^2)^3}} w(\mathbf{p}_A; \mathbf{p}_A^0, \mathbf{X}_A, 0; \sigma_A) \\ &\times w(\mathbf{p}_B; \mathbf{p}_B^0, \mathbf{X}_B, 0; \sigma_B) a(\mathbf{p}_A)^\dagger_A a(\mathbf{p}_B)^\dagger_B |0\rangle. \end{aligned} \quad (2.7)$$

The final state is composed of two particles, C and D , which are the wave packets. The final state is defined in the form

$$\begin{aligned} |\text{final}\rangle &= \int \frac{d^3 p_C}{\sqrt{(2\pi\sigma_C^2)^3}} \int \frac{d^3 p_D}{\sqrt{(2\pi\sigma_D^2)^3}} w(\mathbf{p}_C; \mathbf{p}_C^0, \mathbf{X}_C, T_C; \sigma_C) \\ &\times w(\mathbf{p}_D; \mathbf{p}_D^0, \mathbf{X}_D, T_D; \sigma_D) a(\mathbf{p}_C)^\dagger_C a(\mathbf{p}_D)^\dagger_D |0\rangle. \end{aligned} \quad (2.8)$$

In the above equations, $\mathbf{X}_A, \mathbf{X}_B, \mathbf{X}_C$ and \mathbf{X}_D are the center positions of the wave packets, and $\mathbf{p}_A^0, \mathbf{p}_B^0, \mathbf{p}_C^0$ and \mathbf{p}_D^0 are the central values of momentum of the particles A, B, C and D , respectively. We consider the spatial sizes of the wave packets, $\sigma_{xL} \equiv 1/(2\sigma_L)$ ($L = A, B, C, D$), to be between a macroscopic size and a microscopic size.

In the amplitude Eq. (2.5), the particles A, B, C and D represent directly observed particles. The particle I represent a scalar neutrino and appears only in the intermediate state. Substituting $H_{\text{int}}(t)$, the amplitude is given by

$$S \equiv \langle \text{final} | S[t = T_D, t = 0] | \text{initial} \rangle = \frac{1}{2} F_1 F_2 \sin 2\theta (S_1 - S_2), \quad (2.9)$$

where

$$S_i = \left\{ \prod_{L=A,B,C,D} \int \frac{d^3 p_L}{\sqrt{(2\pi\sigma_L^2)^3}} \right\} \int \frac{d^3 k}{(2\pi)^3} 2E_i \int_0^{T_D} dt_2 \int_0^{t_2} dt_1 \int d^3 x_2 \int d^3 x_1 \\ \times e^{i(p_D - k_i - p_B)x_2 + i(p_C + k_i - p_A)x_1} w_A w_B w_C^* w_D^*. \quad (2.10)$$

From this amplitude, we study neutrino oscillation in the intermediate state. Because the neutrino interacts with matter extremely weakly, it is not observed directly in real experiments. Hence, the amplitudes of the present situation agree with the amplitudes of the realistic experimental situations.

Now we perform the integrations over \mathbf{p}_A , \mathbf{p}_B , \mathbf{p}_C and \mathbf{p}_D in Eq. (2.10). To integrate these variables, the energy is expanded around its central value,

$$E_L(\mathbf{p}) = E_L(\mathbf{p}_L^0) + (\mathbf{p} - \mathbf{p}_L^0) \cdot \mathbf{v}_L, \\ \mathbf{v}_L = \frac{\partial E_L(\mathbf{p}_L^0)}{\partial \mathbf{p}_L}, \quad (2.11)$$

where \mathbf{v}_L is the velocity of the particle L at this momentum, and the momentum integration is carried out as Gaussian integrations. After similar integrations over \mathbf{x}_1 , \mathbf{x}_2 and \mathbf{k} , the transition amplitude is obtained as

$$S_i = N \exp \left[-\frac{\Delta \mathbf{P}^2}{2\sigma^2} \right] \int_0^{T_D} dt_2 \int_0^{t_2} dt_1 \exp \left[-\frac{1}{2} Z_i(t_1, t_2, T_D) + it_1 \Delta \tilde{E}_{1i}^0 + it_2 \Delta \tilde{E}_{2i}^0 \right], \quad (2.12)$$

where

$$N = \left(\frac{2\pi}{\sigma^2} \right)^{3/2} e^{i\phi}, \quad (2.13)$$

$$\phi = -\mathbf{X}_A \cdot \tilde{\mathbf{p}}_A^0 - \mathbf{X}_B \cdot \tilde{\mathbf{p}}_B^0 + (\mathbf{X}_C \cdot \tilde{\mathbf{p}}_C^0 - T_C \tilde{E}_C^0) + (\mathbf{X}_D \cdot \tilde{\mathbf{p}}_D^0 - T_D \tilde{E}_D^0). \quad (2.14)$$

The quantity Z_i in the exponent causes the amplitudes S_i to have dominant contributions from the regions $Z_i \simeq 0$ and is called a ‘‘trajectory function’’. The trajectory functions

$$Z_i(t_1, t_2, T_D) = \frac{\sigma_{AC}^2 \sigma_{BD}^2}{\sigma^2} \mathbf{F}_i^2(t_1, t_2, T_D) + \frac{\sigma_B^2 \sigma_D^2}{\sigma_{BD}^2} \mathbf{G}^2(t_2, T_D) + \frac{\sigma_A^2 \sigma_C^2}{\sigma_{AC}^2} \mathbf{H}^2(t_1), \quad (2.15)$$

$$\mathbf{F}_i(t_1, t_2, T_D) = \mathbf{x}_2^0(t_2, T_D) - \mathbf{x}_1^0(t_1) - \mathbf{v}_i(t_2 - t_1), \quad (2.16)$$

$$\mathbf{G}(t_2, T_D) = \mathbf{X}_D - \mathbf{X}_B - t_2 \mathbf{v}_B - (T_D - t_2) \mathbf{v}_D, \quad (2.17)$$

$$\mathbf{H}(t_1) = \mathbf{X}_C - \mathbf{X}_A - t_1 \mathbf{v}_A - (T_C - t_1) \mathbf{v}_C \quad (2.18)$$

give a classical particle picture, where \mathbf{v}_i is the velocity of I_i and is defined in the same way as (2.11). Here we use for conciseness $\sigma^2 = \sigma_A^2 + \sigma_B^2 + \sigma_C^2 + \sigma_D^2$ and $\sigma_{ij}^2 = \sigma_i^2 + \sigma_j^2$

($i, j = A, B, C, D$). The coefficient of $\mathbf{F}_i^2(t_1, t_2, T_D)$, $\sigma_{AC}^2 \sigma_{BD}^2 / \sigma^2$, is the width of the Gaussian function for the intermediate particle's momentum. In our approach, the intermediate particles become wave packets automatically and then sizes are given by those of the external particles.

The momenta and energies appearing in ϕ are given by,

$$\Delta \mathbf{P} = \mathbf{p}_C^0 + \mathbf{p}_D^0 - \mathbf{p}_A^0 - \mathbf{p}_B^0, \quad (2.19)$$

$$\tilde{\mathbf{p}}_L^0 = \mathbf{p}_L^0 + \frac{\sigma_L^2}{\sigma^2} \Delta \mathbf{P} \quad \text{for } L = A, B \quad (2.20)$$

$$\tilde{\mathbf{p}}_L^0 = \mathbf{p}_L^0 - \frac{\sigma_L^2}{\sigma^2} \Delta \mathbf{P} \quad \text{for } L = C, D, \quad (2.21)$$

$$\tilde{E}_L^0 = E_L^0 + \frac{\sigma_L^2}{\sigma^2} \mathbf{v}_L \cdot \Delta \mathbf{P}, \quad \text{for } L = A, B \quad (2.22)$$

$$\tilde{E}_L^0 = E_L^0 - \frac{\sigma_L^2}{\sigma^2} \mathbf{v}_L \cdot \Delta \mathbf{P}, \quad \text{for } L = C, D \quad (2.23)$$

$$\Delta \tilde{E}_{1i}^0 = \tilde{E}_C^0 + E_i(\mathbf{k}^0) - \tilde{E}_A^0, \quad (2.24)$$

$$\Delta \tilde{E}_{2i}^0 = \tilde{E}_D^0 - E_i(\mathbf{k}^0) - \tilde{E}_B^0. \quad (2.25)$$

The quantity $-\Delta \mathbf{P}^2 / (2\sigma^2)$ in the exponent of Eq. (2.12) is called the ‘‘momentum function’’. It gives a constraint on the differences between momenta.

The intermediate particles appear as wave packets even if they were not originally prepared as wave packets, and their momenta are given by the following function of the momenta of external particles :

$$\mathbf{k}^0 = \mathbf{p}_D^0 - \mathbf{p}_B^0 - \frac{\sigma_{BD}^2}{\sigma^2} \Delta \mathbf{P}. \quad (2.26)$$

\mathbf{x}_1^0 and \mathbf{x}_2^0 are the central positions of the interaction vertices and written

$$\mathbf{x}_1^0(t_1) = \frac{1}{\sigma_{AC}^2} \left\{ \sigma_A^2 (\mathbf{X}_A + t_1 \mathbf{v}_A) + \sigma_C^2 (\mathbf{X}_C - (T_C - t_1) \mathbf{v}_C) \right\}, \quad (2.27)$$

$$\mathbf{x}_2^0(t_2, T_D) = \frac{1}{\sigma_{BD}^2} \left\{ \sigma_B^2 (\mathbf{X}_B + t_2 \mathbf{v}_B) + \sigma_D^2 (\mathbf{X}_D - (T_D - t_2) \mathbf{v}_D) \right\}. \quad (2.28)$$

The Gaussian term in Eq. (2.12) places the constraint $\mathbf{p}_C^0 + \mathbf{p}_D^0 - \mathbf{p}_A^0 - \mathbf{p}_B^0 \approx 0$ on the momentum with the width $\sqrt{2\sigma^2}$. The momentum is approximately conserved, because the initial state and final state are approximate eigenstates of the momentum. The Gaussian terms in the integrand of S_i place the constraints $\mathbf{F}_i \approx 0$, $\mathbf{G} \approx 0$ and $\mathbf{H} \approx 0$ on to the times t_1 and t_2 . These correspond to the classical trajectories in the particle picture. The latter constraints become stronger as the spatial sizes of the wave packets become smaller.

§3. Gaussian approximation in time integration

In this section we study the amplitude Eq. (2·12) further. In order to perform the time integrations, the exponent of the integrand in Eq. (2·12) is rewritten as follows

$$\begin{aligned}
& -\frac{1}{2}Z_i(t_1, t_2, T_D) + it_1\Delta\tilde{E}_{1i}^0 + it_2\Delta\tilde{E}_{2i}^0 = -\frac{1}{2}Z_i(t_{1i}^0, t_{2i}^0, T_D) + it_{1i}^0(T_D)\Delta\tilde{E}_{1i}^0 + it_{2i}^0(T_D)\Delta\tilde{E}_{2i}^0 \\
& -\frac{1}{2\bar{\sigma}_{t_{1i}}^2} \left(t_1 - t_{1i}^0(T_D) - \frac{\Delta t_{1i}^0}{\bar{\sigma}_{t_{2i}}} (t_2 - t_{2i}^0(T_D)) - i\bar{\sigma}_{t_{1i}}^2 \Delta\tilde{E}_{1i}^0 \right)^2 \\
& -\frac{1}{2\bar{\sigma}_{t_{2i}}^2} \left(t_2 - t_{2i}^0(T_D) - i\bar{\sigma}_{t_{2i}} (\bar{\sigma}_{t_{2i}} \Delta\tilde{E}_{2i}^0 + \Delta t_{1i}^0 \Delta\tilde{E}_{1i}^0) \right)^2 \\
& -\frac{1}{2} \left(\bar{\sigma}_{t_{1i}} \Delta\tilde{E}_{1i}^0 \right)^2 - \frac{1}{2} \left(\bar{\sigma}_{t_{2i}} \Delta\tilde{E}_{2i}^0 + \Delta t_{1i}^0 \Delta\tilde{E}_{1i}^0 \right)^2, \tag{3·1}
\end{aligned}$$

where $\bar{\sigma}_{t_{1i}}^2$ and $\bar{\sigma}_{t_{2i}}^2$ are the widths of t_1 and t_2 and are given as

$$\frac{1}{\bar{\sigma}_{t_{1i}}^2} = \frac{1}{2} \left(\frac{\partial^2 Z_i}{\partial t_1^2} \right), \tag{3·2}$$

$$\frac{1}{\bar{\sigma}_{t_{2i}}^2} = \frac{1}{2} \left(\frac{\partial^2 Z_i}{\partial t_2^2} \right) - \frac{1}{4} \bar{\sigma}_{t_{1i}}^2 \left(\frac{\partial^2 Z_i}{\partial t_1 \partial t_2} \right)^2, \tag{3·3}$$

$$\Delta t_{1i}^0 = -\frac{1}{2} \bar{\sigma}_{t_{1i}}^2 \left(\frac{\partial^2 Z_i}{\partial t_1 \partial t_2} \right) \bar{\sigma}_{t_{2i}}, \tag{3·4}$$

and $t_{1i}^0(T)$ and $t_{2i}^0(T)$ are regarded as the central values of the time of interactions and are defined by

$$\begin{aligned}
\left. \frac{\partial Z_i}{\partial t_1} \right|_{\substack{t_1=t_{1i}^0 \\ t_2=t_{2i}^0}} &= 0, \\
\left. \frac{\partial Z_i}{\partial t_2} \right|_{\substack{t_1=t_{1i}^0 \\ t_2=t_{2i}^0}} &= 0. \tag{3·5}
\end{aligned}$$

Because the explicit forms of $t_{1i}^0(T_D)$, $t_{2i}^0(T_D)$, $\bar{\sigma}_{t_{1i}}^2$, $\bar{\sigma}_{t_{2i}}^2$ and Δt_{1i}^0 are quite complicated, we just give quadratic forms of the trajectory function, and the explicit forms are given in Appendix A. Here the central values of the times and time widths depend on the momenta of the external and internal particles. Therefore it happens in some situations that time widths become very large, although the spatial widths of external particles are finite.

The amplitude S_i is given by

$$\begin{aligned}
S_i &= N \exp \left[-\frac{1}{2}Z_i(t_{1i}^0, t_{2i}^0, T_D) - \frac{\Delta \mathbf{P}^2}{2\sigma^2} - \frac{1}{2} \left(\bar{\sigma}_{t_{1i}} \Delta\tilde{E}_{1i}^0 \right)^2 - \frac{1}{2} \left(\bar{\sigma}_{t_{2i}} \Delta\tilde{E}_{2i}^0 + \Delta t_{1i}^0 \Delta\tilde{E}_{1i}^0 \right)^2 \right] \\
&\times \exp \left[it_{1i}^0(T_D)\Delta\tilde{E}_{1i}^0 + it_{2i}^0(T_D)\Delta\tilde{E}_{2i}^0 \right]
\end{aligned}$$

$$\begin{aligned}
& \times \int_0^{T_D} dt_2 \exp \left[-\frac{1}{2\bar{\sigma}_{t_2}^2} \left(t_2 - t_{2i}^0(T_D) - i\bar{\sigma}_{t_2} (\bar{\sigma}_{t_2} \Delta\tilde{E}_{2i}^0 + \Delta t_{1i}^0 \Delta\tilde{E}_{1i}^0) \right)^2 \right] \\
& \times \int_0^{t_2} dt_1 \exp \left[-\frac{1}{2\bar{\sigma}_{t_1}^2} \left(t_1 - t_{1i}^0(T_D) - \frac{\Delta t_{1i}^0}{\bar{\sigma}_{t_2}} (t_2 - t_{2i}^0(T_D)) - i\bar{\sigma}_{t_1}^2 \Delta\tilde{E}_{1i}^0 \right)^2 \right]. \quad (3.6)
\end{aligned}$$

From the integrand in Eq. (3.6), we find that the integrations over t_1 and t_2 are separated when both time widths $\bar{\sigma}_{t_1}^2$ and $\bar{\sigma}_{t_2}^2$ are small enough compared to the time interval T_D . Afterwards, we assume that these conditions are satisfied. Then we can integrate Eq. (3.6) over t_1 and t_2 , and we obtain

$$\begin{aligned}
S_i &= 2\pi N \sqrt{\bar{\sigma}_{t_1}^2 \bar{\sigma}_{t_2}^2} \times \exp \left[it_{1i}^0(T_D) \Delta\tilde{E}_{1i}^0 + it_{2i}^0(T_D) \Delta\tilde{E}_{2i}^0 \right] \\
& \times \exp \left[-\frac{1}{2} Z_i(t_{1i}^0, t_{2i}^0, T_D) - \frac{\Delta\mathbf{P}^2}{2\sigma^2} - \frac{1}{2} \left(\bar{\sigma}_{t_1} \Delta\tilde{E}_{1i}^0 \right)^2 - \frac{1}{2} \left(\bar{\sigma}_{t_2} \Delta\tilde{E}_{2i}^0 + \Delta t_{1i}^0 \Delta\tilde{E}_{1i}^0 \right)^2 \right]. \quad (3.7)
\end{aligned}$$

The quantity $\sqrt{\bar{\sigma}_{t_1}^2 \bar{\sigma}_{t_2}^2}$ appears as an overall factor in a consequence of the time integrations. The amplitudes become large when the time widths are large. This factor is derived only in a field theoretical treatment in which whole process is involved.

In the second line of Eq. (3.7), the contribution from the trajectory function to the amplitudes becomes maximal at t_{1i}^0 and t_{2i}^0 . Here, t_{1i}^0 is the central value of the production time of I_i , and t_{2i}^0 is that of the detection time. The Gaussian integration with t_{1i}^0 and t_{2i}^0 in Eq. (3.6) becomes negligible, unless the condition

$$0 < t_{1i}^0(T_D) < t_{2i}^0(T_D) < T_D. \quad (3.8)$$

is satisfied.

We see from Eq. (3.7) that the phase difference Θ_{21} up to $\mathcal{O}(m^2)$ can be expressed in the form

$$\Theta_{21}(T) = -\frac{\Delta m_{21}^2}{2|\mathbf{k}^0|} (t_2^0(T_D) - t_1^0(T_D)) + \Delta m_{21}^2 \left(\Delta\tilde{E}_1^0 \frac{\partial t_{1i}^0}{\partial m_i^2} \Big|_{m_i=0} + \Delta\tilde{E}_2^0 \frac{\partial t_{2i}^0}{\partial m_i^2} \Big|_{m_i=0} \right), \quad (3.9)$$

where t_1^0 , t_2^0 , $\Delta\tilde{E}_1^0$ and $\Delta\tilde{E}_2^0$ are the central times and energy differences with $m_i = 0$.

The first term of Eq. (3.9) corresponds to the phase of the standard formula, and the second term results from the field theoretical treatment. The phase difference takes a form similar to that of the standard formula when $\Delta\tilde{E}_1^0$, $\Delta\tilde{E}_2^0$ and $\Delta\mathbf{P}$ are zero. In this case, we have the standard formula when $t_2^0 - t_1^0$ can be regarded as the travel time of the neutrinos. However, t_2^0 is different from the final time T_D , and t_1^0 is different from the initial time, and they are given by Eq. (3.5). Thus, our formula is not exactly the same as the standard formula.

The absolute square of the amplitude, $|S|^2$, gives the transition probability from the initial state (2-7), which is prepared at $t = 0$ to the final state (2-8), which is measured at $t = T_D$. In observations of solar neutrinos and atmospheric neutrinos, the detection time is not measured. In baseline neutrino experiments, the detection time is measured but with finite precision. Therefore we have to sum up $|S|^2$ in a finite detection time. Here we make the assumption that the measurements at different times are independent phenomena. This assumption is consistent with the definition of wave packet states that they are defined with infinite precision and with the fact that the event rate is very small. From this assumption, we can integrate $|S|^2$ over the detection time T_D :

$$|\tilde{S}|^2 = \int dT_D |S|^2. \quad (3.10)$$

The integration interval is different for different situations. It is from 0 to ∞ for neutrinos from the sun or atmosphere, and from $T_D - \Delta T_D/2$ to $T_D + \Delta T_D/2$ for baseline neutrino oscillation experiments, where ΔT_D is the resolution of the detection time.

We assume that the Gaussian approximation is valid for the T_D integral. Then, the transition probability becomes

$$\begin{aligned} |\tilde{S}|^2 = & \sum_{i=1,2} \sqrt{\bar{\sigma}_{T_D i}^2} C_i^2 \exp[2A_i] - 2C_1 C_2 \sqrt{\frac{2\bar{\sigma}_{T_D 1}^2 \bar{\sigma}_{T_D 2}^2}{\bar{\sigma}_{T_D 1}^2 + \bar{\sigma}_{T_D 2}^2}} \\ & \times \exp \left[A_1 + A_2 - \frac{(T_{D2}^0 - T_{D1}^0)^2}{2(\bar{\sigma}_{T_D 1}^2 + \bar{\sigma}_{T_D 2}^2)} - \frac{1}{2} \bar{\sigma}_{T_D}^2 \left(\frac{\partial \Theta_{21}(T_D)}{\partial T_D} \right)^2 \right] \cos(\Theta_{21}(\tilde{T}_D^0)), \end{aligned} \quad (3.11)$$

where A_i represents the energy and momentum functions and trajectory function, and $\bar{\sigma}_{T_D i}^2$ represents the width of the detection time, T_D . These are given by

$$C_i = (2\pi)^{5/2} (\sigma^2)^{-3/2} (\bar{\sigma}_{t_{1i}}^2 \bar{\sigma}_{t_{2i}}^2)^{1/2} \frac{1}{E_i},$$

$$A_i = -\frac{1}{2} Z_i(t_{1i}^0, t_{2i}^0, T_{Di}^0) - \frac{\Delta \mathbf{P}^2}{2\sigma^2} - \frac{1}{2} \left(\bar{\sigma}_{t_{1i}} \Delta \tilde{E}_{1i}^0 \right)^2 - \frac{1}{2} \left(\bar{\sigma}_{t_{2i}} \Delta \tilde{E}_{2i}^0 + \Delta t_{1i}^0 \Delta \tilde{E}_{1i}^0 \right)^2, \quad (3.12)$$

$$\bar{\sigma}_{T_D} = \sqrt{\frac{\bar{\sigma}_{T_D 1}^2 \bar{\sigma}_{T_D 2}^2}{\bar{\sigma}_{T_D 1}^2 + \bar{\sigma}_{T_D 2}^2}}, \quad (3.13)$$

$$\frac{1}{\bar{\sigma}_{T_D i}^2} = \frac{1}{2} \left(\frac{\partial^2 Z_i}{\partial T_D^2} \right). \quad (3.14)$$

The quantity Θ_{21} is the phase difference between I_1 and I_2 in Eq. (3-9). The detection time is replaced by its central value,

$$\tilde{T}_D^0 = \frac{\bar{\sigma}_{T_D 1}^2 T_{D2}^0 + \bar{\sigma}_{T_D 2}^2 T_{D1}^0}{\bar{\sigma}_{T_D 1}^2 + \bar{\sigma}_{T_D 2}^2},$$

where $T_{D_i}^0$ is the central value of the detection time in which only the mass eigenstate I_i appears as the intermediate state, and it is defined by

$$\left. \frac{\partial Z_i}{\partial T_D} \right|_{T_D=T_{D_i}^0} = 0. \quad (3.15)$$

In the exponent of the second term in Eq. (3.11), last two terms are characteristic terms in wave-packet treatment. One is called the ‘‘decoherence function’’, which represents an overlap in the detection time through two intermediate states :

$$\text{Decoherence function} = -\frac{(T_{D2}^0 - T_{D1}^0)^2}{2(\bar{\sigma}_{T_{D1}}^2 + \bar{\sigma}_{T_{D2}}^2)}. \quad (3.16)$$

When the detection time difference, $T_{D2}^0 - T_{D1}^0$, becomes larger than the detection time width, $\sqrt{\bar{\sigma}_{T_{D1}}^2 + \bar{\sigma}_{T_{D2}}^2}$, the oscillation disappears, because the coherence in the time direction is lost. The other is called the ‘‘phase function’’, which gives the condition that the detection time width must be smaller than the oscillation period :

$$\begin{aligned} \text{Phase function} &= -\frac{1}{2}\bar{\sigma}_{T_D}^2 \left(\frac{\partial \Theta_{21}(T_D)}{\partial T_D} \right)^2 \\ &= -\frac{1}{2} \left(\frac{\bar{\sigma}_{T_D}}{T_D^{\text{osc}}} \right)^2 (2\pi - \Theta_{21}(0))^2. \end{aligned} \quad (3.17)$$

Here T_D^{osc} is a period and is defined by $\Theta_{21}(T_D^{\text{osc}}) = 2\pi$. The extra coefficient $2\pi - \Delta\Theta(0)$ appears due to the field theoretical treatment.

The energy function places a constraint on the energy differences $\Delta\tilde{E}_{1i}^0$ and $\Delta\tilde{E}_{2i}^0$,

$$-\frac{1}{2} \left(\bar{\sigma}_{t_{1i}} \Delta\tilde{E}_{1i}^0 \right)^2 - \frac{1}{2} \left(\bar{\sigma}_{t_{2i}} \Delta\tilde{E}_{2i}^0 + \Delta t_{1i}^0 \Delta\tilde{E}_{1i}^0 \right)^2. \quad (3.18)$$

Energy conservation is satisfied when the energy function is zero.

When the energy-momentum and the trajectory functions in one dimension are zero, the phase difference, Eq. (3.9), becomes

$$\Theta_{21}(\tilde{T}_D^0) = \frac{\Delta m_{21}^2}{2|\mathbf{k}^0|} (X_B - X_A + t_2^0(\tilde{T}_D^0)v_B - t_1^0(\tilde{T}_D^0)v_A). \quad (3.19)$$

Equation (3.19) agrees with the phase of the standard formula^{9),10)} if $t_2^0 v_B$ and $t_1^0 v_A$ are negligible.

§4. The effect of a finite lifetime on the wave packets

In this section, we study the transition amplitude and probability when a source particle has a finite lifetime. *) From these, the particle oscillation of the intermediate particle is

*) This includes cases in which a particle is stable but the state loses the quantum mechanical coherence after a finite time. The τ stands for the relaxation time in this case.

studied.

The finite lifetime τ is introduced for the particle A in the following manner. The field operator of the particle A, Φ_A , contains $\Gamma = 1/\tau$ as

$$\Phi_A(x) = \int \frac{d^3p}{2E_A} \exp(i\mathbf{p} \cdot \mathbf{x} - i(E_A - i\Gamma/2)t) a(\mathbf{p})_A + h.c. \quad (4.1)$$

In consequence of this addition in Eq. (2.12), a damping factor $-\Gamma/2$ is added to $E_A(p_A^0)$ in the previous section. In this section, we study the amplitude and probability in the case that both widths $\bar{\sigma}_{t_2}$ and $\bar{\sigma}_{t_1}$ are small enough compared to the time interval T_D and the lifetime τ satisfies $\tau \gg \bar{\sigma}_{t_1}$ and $\bar{\sigma}_{t_2}$. Then, as in the previous section, it has been found that the integrations over t_1 and t_2 in the amplitudes are separated.

If these conditions are not satisfied, the Gaussian approximation is invalid, and the integrations over t_1 and t_2 cannot be separated. Then, the calculation would be similar to that for in plane waves. Below, we assume that these conditions are satisfied. Therefore the transition amplitude given by Eq. (3.6) are modified into the following form:

$$S = \frac{1}{2}F_1F_2 \sin 2\theta(S_1 - S_2), \quad (4.2)$$

where

$$S_i = 2\pi N \sqrt{\bar{\sigma}_{t_{1i}}^2 \bar{\sigma}_{t_{2i}}^2} \times \exp \left[it_{1i}^{0'}(T_D) \Delta \tilde{E}_{1i}^0 + it_{2i}^{0'}(T_D) \Delta \tilde{E}_{2i}^0 - t_{1i}^{0'} \frac{\Gamma}{2} \right] \\ \times \exp \left[-\frac{1}{2} Z_i(t_{1i}^{0'}, t_{2i}^{0'}, T_D) - \frac{\Delta \mathbf{P}^2}{2\sigma^2} - \frac{1}{2} \left(\bar{\sigma}_{t_{1i}} \Delta \tilde{E}_{1i}^0 \right)^2 - \frac{1}{2} \left(\bar{\sigma}_{t_{2i}} \Delta \tilde{E}_{2i}^0 + \Delta t_{1i}^0 \Delta \tilde{E}_{1i}^0 \right)^2 \right]. \quad (4.3)$$

The new central times $t_{1i}^{0'}$ and $t_{2i}^{0'}$ of the Gaussian functions of t_1 and t_2 in Eq. (4.3) are obtained from old ones in Eq. (3.5) as follows

$$t_{1i}^{0'}(T_D) = t_{1i}^0(T_D) - (\bar{\sigma}_{t_{1i}}^2 + \Delta t_{1i}^{0\prime 2}) \frac{\Gamma}{2}, \quad (4.4)$$

$$t_{2i}^{0'}(T_D) = t_{2i}^0(T_D) - \bar{\sigma}_{t_{2i}} \Delta t_{1i}^0 \frac{\Gamma}{2}. \quad (4.5)$$

The transition probability is also calculated by assuming the Gaussian approximation for T_D integration. It is given by

$$|\tilde{S}|^2 = \sum_{i=1,2} \sqrt{\bar{\sigma}_{T_D i}^2 \tilde{S}_i^2} - 2 \sqrt{\frac{2\bar{\sigma}_{T_D 1}^2 \bar{\sigma}_{T_D 2}^2}{\bar{\sigma}_{T_D 1}^2 + \bar{\sigma}_{T_D 2}^2}} \tilde{S}_1 \tilde{S}_2 \\ \times \exp \left[-\frac{(T_{D2}^{0'} - T_{D1}^{0'})^2}{2(\bar{\sigma}_{T_D 1}^2 + \bar{\sigma}_{T_D 2}^2)} - \frac{1}{2} \bar{\sigma}_{T_D}^2 \left(\frac{\partial \Theta'_{21}(T_D)}{\partial T_D} \right)^2 \right] \cos(\Theta'_{21}(\tilde{T}_D^0)), \quad (4.6)$$

$$\tilde{S}_i = C_i \exp \left[A_i' - \frac{\Gamma}{2} t_{1i}^{0'}(T_{D_i}^0) \right], \quad (4.7)$$

where the coefficients C_i are the same as before. $T_{Di}^{0'}$ is the central time of the detection time and is given by

$$T_{Di}^{0'} = T_{Di}^0 - \frac{\Gamma}{2} \bar{\sigma}_{T_{Di}}^2 \left(\frac{\partial t_{1i}^{0'}(T_D)}{\partial T_D} \right). \quad (4.8)$$

Θ'_{21} and A'_i are obtained by replacing t_{1i}^0 , t_{2i}^0 and T_{Di}^0 by $t_{1i}^{0'}$, $t_{2i}^{0'}$ and $T_{Di}^{0'}$ in Eq. (3-9) and (3-12). The Gaussian approximation for t_1 and t_2 is useful and is valid when $\tau \gg \bar{\sigma}_{t_{1i}}^2$, $\bar{\sigma}_{t_{2i}}^2$ is satisfied. This condition is satisfied for a lifetime $\tau = 10^{-8}$ sec of the pion and σ_{xL} ($L = A, B, C, D$) of atomic size.

We see from Eqs. (3-11) and (4-6) that the exponential in the oscillation term becomes maximum at the given positions X_i when the energy-momentum function and the trajectory function vanish. However the peak of the oscillation probability does not always coincide with that of the exponential, because of the coefficient and the lifetime. The lifetime and relaxation time reduce the magnitude of the oscillation probability depending on how long the particle A lives. If the constraints from energy-momentum conservation and the classical trajectories are weak, the oscillation probabilities become maximal at the position where the energy and momentum are not conserved. Then, as a result, the oscillation length changes from that of the standard formula. Such situations seem quite strange. However as we show below, these phenomena occur when the spatial widths of the external particles are extremely small, on the order of 1 fm.

§5. Coherence conditions

Here we examine necessary conditions for oscillation of an intermediate particles to take place, based on the transition probabilities Eq. (3-11) and (4-6). Oscillation occurs when the interference term of two amplitudes becomes finite. Two amplitudes have peaks in different positions and decrease rapidly, so the interference term becomes finite only when the peak position overlaps within the widths. We find these conditions, coherent conditions, in the present section. There exist several previous works on this topic,^{3)-7)12),13)} but our results based on field theory are different from them. In our method, the coherence conditions are written in terms of measured quantities, like the positions, velocities and wave packet sizes for external particles.

5.1. Energy function

The factor

$$\exp \left[-\frac{1}{2} \left(\bar{\sigma}_{t_{1i}} \Delta \tilde{E}_{1i}^0 \right)^2 - \frac{1}{2} \left(\bar{\sigma}_{t_{2i}} \Delta \tilde{E}_{2i}^0 + \Delta t_{1i}^0 \Delta \tilde{E}_{1i}^0 \right)^2 \right], \quad (5.1)$$

which also appears in the amplitude S_i , yields the approximate energy conservation and imposes the constraint on Δm_{21}^2 and σ_x to generate oscillations. The Gaussian function (5.1) has a width $\bar{\sigma}_{t_{1i}}^2$ of $\Delta\tilde{E}_{1i}$ and $\bar{\sigma}_{t_{2i}}^2$ of $\Delta\tilde{E}_{2i} + \frac{\Delta t_{1i}^0}{\bar{\sigma}_{t_{2i}}} \Delta\tilde{E}_{1i}$. Note that the second term in (5.1) contains $\Delta\tilde{E}_{1i}$ because of finite interaction time interval. We understand from these terms that when $\Delta\tilde{E}_{12} - \Delta\tilde{E}_{11}$ or $\Delta\tilde{E}_{22} - \Delta\tilde{E}_{21}$ becomes larger than $(\bar{\sigma}_{t_{1i}})^{-1}$ or $(\bar{\sigma}_{t_{2i}} - \Delta t_{1i})^{-1}$, the interference of I_1 and I_2 disappears, and the oscillation does not take place. From Eqs. (2.24) and (2.25), $\Delta\tilde{E}_{12} - \Delta\tilde{E}_{11} = \frac{\Delta m_{21}^2}{2|\mathbf{k}^0|}$ and $\Delta\tilde{E}_{22} - \Delta\tilde{E}_{21} = -\frac{\Delta m_{21}^2}{2|\mathbf{k}^0|}$, this coherence condition for oscillations is reduced to

$$\begin{aligned}\frac{\Delta m_{21}^2}{2E} &\leq \frac{1}{|\bar{\sigma}_{t_1}|}, \\ \frac{\Delta m_{21}^2}{2E} &\leq \frac{1}{|\bar{\sigma}_{t_2} - \Delta t_1|},\end{aligned}\tag{5.2}$$

where E represents $|\mathbf{k}^0|$ and $\bar{\sigma}_{t_1}$, $\bar{\sigma}_{t_2}$ and Δt_1 are the values of Eq. (3.2)–(3.4) at $m_i = 0$. The above coherence conditions (5.2) are expressed as

$$\frac{2\pi}{L_{\text{osc}}} \leq \frac{1}{|\bar{\sigma}_{t_1}|}, \quad \text{or} \quad \frac{1}{|\bar{\sigma}_{t_2} - \Delta t_1|},\tag{5.3}$$

where $L_{\text{osc}} = \frac{4\pi E}{\Delta m_{21}^2}$ is the oscillation length in the standard oscillation formula, which is almost the same as that derived from (3.19). Using the spatial widths $\bar{\sigma}_{x_1}$ and $\bar{\sigma}_{x_2}$ of intermediate particles in the production and detection processes defined by

$$\begin{aligned}\bar{\sigma}_{x_1} &\equiv v_I |\bar{\sigma}_{t_1}|, \\ \bar{\sigma}_{x_2} &\equiv v_I |\bar{\sigma}_{t_2} - \Delta t_1|,\end{aligned}\tag{5.4}$$

where v_I is the velocity of the intermediate particle and is equal to 1, Eqs. (5.3) is written as

$$\bar{\sigma}_{x_1}, \bar{\sigma}_{x_2} \leq \frac{L_{\text{osc}}}{2\pi}\tag{5.5}$$

for standard oscillations to take place. When the above constraints are not satisfied, ordinary interference of I_1 and I_2 does not exist, and the oscillation disappears. Consequently, the transition probability becomes constant in the time interval T_D .

5.2. Trajectory function

The trajectory functions in each amplitude, S_i ,

$$\begin{aligned}&\exp\left[-\frac{1}{2}Z_i(t_{1i}^0, t_{2i}^0, T_{Di}^0)\right] \\ &= \exp\left[-\frac{\sigma_{AC}^2 \sigma_{BD}^2}{2\sigma^2} \mathbf{F}_i^2(t_{1i}^0, t_{2i}^0, T_{Di}^0) - \frac{\sigma_B^2 \sigma_D^2}{2\sigma_{BD}^2} \mathbf{G}^2(t_{2i}^0, T_{Di}^0) - \frac{\sigma_A^2 \sigma_C^2}{2\sigma_{AC}^2} \mathbf{H}^2(t_{1i}^0)\right],\end{aligned}\tag{5.6}$$

also give necessary constraints for oscillation to take place. These forms are very complicated, and it is difficult to find expressions using parameters of external particles. For this reason, we express constraints using the center times and the center positions. These conditions are given as

$$|\delta\mathbf{F}| \equiv |\mathbf{F}_2 - \mathbf{F}_1| \leq \sqrt{\frac{\sigma^2}{\sigma_{AC}^2 \sigma_{BD}^2}}, \quad (5.7)$$

$$|\delta\mathbf{G}| \equiv |\mathbf{G}_2 - \mathbf{G}_1| \leq \sqrt{\frac{\sigma_{BD}^2}{\sigma_B^2 \sigma_D^2}}, \quad (5.8)$$

$$|\delta\mathbf{H}| \equiv |\mathbf{H}_2 - \mathbf{H}_1| \leq \sqrt{\frac{\sigma_{AC}^2}{\sigma_A^2 \sigma_C^2}}. \quad (5.9)$$

From Eqs. (2.16) to (2.18), the above constraints are rewritten as

$$\left| \delta\mathbf{x}_2^0 - \delta\mathbf{x}_1^0 - \hat{\mathbf{k}}(\delta t_2^0 - \delta t_1^0) + \frac{\Delta m_{21}^2}{2E^2} \hat{\mathbf{k}}(t_2^0(T_{Di}^0) - t_1^0(T_{Di}^0)) \right| \leq \sqrt{\frac{\sigma^2}{\sigma_{AC}^2 \sigma_{BD}^2}}, \quad (5.10)$$

$$|(\mathbf{v}_B - \mathbf{v}_D)\delta t_2^0 + \mathbf{v}_D \delta T^0| \leq \sqrt{\frac{\sigma_{BD}^2}{\sigma_B^2 \sigma_D^2}}, \quad (5.11)$$

$$|\mathbf{v}_C - \mathbf{v}_A| |\delta t_1^0| \leq \sqrt{\frac{\sigma_{AC}^2}{\sigma_A^2 \sigma_C^2}}. \quad (5.12)$$

Throughout this section, we write the center times without a prime for the case in which the particle A has a finite lifetime.

The right-hand side of the first constraint, Eq. (5.10) is the spatial width of the intermediate particle, and those of the second and third constraints, Eq. (5.11) and (5.12), are the sums of the spatial widths of the external particles. On the left-hand side of the first condition, $\frac{\Delta m_{21}^2}{2E^2} \hat{\mathbf{k}}(t_2^0 - t_1^0)$ is rewritten as follows

$$\lambda \frac{L_{\text{travel}}}{L_{\text{osc}}} \hat{\mathbf{k}}, \quad (5.13)$$

where $L_{\text{travel}} = t_2^0 - t_1^0$, and λ is the de Broglie wavelength for the intermediate particles. Unless L_{travel} is much larger than L_{osc} , Eq. (5.13) is of order λ or less, and the condition (5.10) is satisfied.

5.3. Decoherence function

The decoherence function Eq. (3.16) appearing in the probabilities (3.11) and (4.6) constrains the difference between the central times of detection time as

$$\delta T_D^0 \leq 2\bar{\sigma}_T. \quad (5.14)$$

Here, $\bar{\sigma}_{T_D}$ is the value of Eq. (3.14) at $m_i = 0$. This constraint gives the “decoherence time” as a function of the detector position, particles velocities and wave packet sizes. Note that in our approach, oscillating particles appear as intermediate, states and only external particles are observed. Therefore the decoherence condition is given for the detection times of the scattering particle, not for the flight distance of intermediate particles. From (5.14), when δT_D^0 is larger than $2\bar{\sigma}_{T_D}$, coherence is lost and no oscillation is seen.

5.4. Phase function

The phase function Eq. (3.17) in the oscillation probability gives a constraint on oscillation period, T_D^{osc} :

$$2(2\pi - \Theta_{21}(0))\bar{\sigma}_{T_D} \leq T_D^{osc}. \quad (5.15)$$

This relation implies that when the oscillation period is smaller than the width of the detection time, the oscillation disappears.

5.5. Lifetime

The lifetime effect from a source particle A is seen explicitly as $\exp(-\Gamma/2t_i^0)$ in the absolute square of the amplitude (4.6). From the right-hand side of (4.7), this term gives constraint

$$\delta t_1^0 \leq \tau. \quad (5.16)$$

From this relation, to maintain coherence, the difference in the production time for intermediate particles must be smaller than the lifetime of the source particle.

§6. The numerical results of transition probabilities

In this section, we give the results for the numerical calculations of the oscillation probabilities. The particle C , which corresponds to a muon in pion decay, usually is not detected in most experiments and observations. From this fact, the oscillation probabilities that we actually measure are the sums of probabilities over \mathbf{p}_C^0 . Therefore, we consider the following probabilities instead**) of those in Eq. (3.11) and Eq. (4.6) :

$$\bar{P}(X_B) = N_{\text{norm}} \int d\mathbf{p}_C^0 |\tilde{S}|^2. \quad (6.1)$$

**) Actually, $|\tilde{S}|^2$ is constant with \mathbf{X}_C in finite macroscopic range. Therefore this value is equivalent to a probability integrated over coordinate

$$\int d\mathbf{p}_C^0 \int d\mathbf{X}_C |\tilde{S}|^2,$$

in which the orthogonality of states with different values of \mathbf{p}_C^0 is satisfied.

Here, $|\tilde{S}|^2$ is given in Eq. (3-11) or (4-6), and N_{norm} is a normalization factor. We investigate the following three situations of different parameters:

1. Intermediate particles are produced by the decay of the particle A in flight. The average momentum of each external particle is taken so that the average momentum of the intermediate particle is about 430 MeV. This case mimics long base line experiments.
2. The intermediate particles are produced by the decay of the particle A at rest. The mass of the particle A is chosen as about 140 MeV, which gives the intermediate particles' momentum as 30 MeV.
3. The intermediate particles are produced by the decay of the heavy particle A in flight. The average momenta of external particles are taken so that the intermediate particles momentum becomes 0.4 MeV.

The first and the second cases correspond to “decay in flight” (DIF) and “decay at rest” (DAR) neutrinos in neutrino oscillation experiments using pion sources. The third case correspond to “solar neutrinos from ${}^7\text{Be}$ decay” whose energies are MeV (low energy or LE).

In baseline experiments, the momenta of source particles are focused in the direction of the detector and the momenta of produced neutrinos and accompanying charged leptons are in almost the same direction. In solar neutrino observations, the velocities of source and accompanying particles are slow, because their momenta are much lower than their masses. Therefore the one-dimensional approximation is valid in the above three cases. For these reasons, we perform \mathbf{p}_C^0 integral in one dimension.

For the numerical calculations, we use the following parameters: $m_1 = 0.1$ eV and $m_2 = 0.2$ eV and $\theta = \frac{\pi}{4}$ in all cases. These are the same values in (I). The wave packet sizes, σ_L ($L = A, B, C, D$), are also taken to be the same. The values of other parameters are given in Table I.

T_C in case 1 and case 2 and X_C in case 3 are not shown in Table.I. We set these parameters by hand as a function of p_C^0 , because there is no way to determine both X_C and T_C in one dimension. The concrete forms of $T_C(p_C^0)$ and $X_C(p_C^0)$ are given in the following subsections.

6.1. Case 1: Decay in flight

In the first case, the particle I is produced by the decay of the particle A in flight accompanying C , and the particle D appears through the interactions between the particle B at rest and I .

In baseline experiments, the particle C is considered to be stopped at a beam dump. Therefore we set X_C to a constant value. But the detection time of C is unknown. Therefore we study the probability of a certain time T_C , which is a function of P_C^0 . T_C should be such

	case 1	case 2	case 3
m_A	140.0	140.0	6.3×10^3
m_B	2.9×10^{-4}	4.2×10^{-3}	2.4×10^{-1}
m_C	106.0	106.0	6.29960×10^3
m_D	0.5	0.5	0.5
p_A^0	1000.0	0.0	1.3
p_B^0	0.0	0.0	0.0
p_D^0	428.8	29.9	0.4
X_A	0.0	0.0	0.0
X_C	300.0	-5.0	—
X_D	$X_B + 1.0 \times 10^{-9}$	$X_B + 1.0 \times 10^{-9}$	$X_B + 1.0 \times 10^{-9}$
T_C	—	—	τ
τ	2.6×10^{-8}	2.6×10^{-8}	1.0×10^{-12}

Table I. The masses m_L and the momenta p_L^0 in MeV, and the positions X_L in meters. The lifetimes or relaxation times, τ are in seconds. ($L = A, B, C, D$)

that the time order for the central times is given by

$$0 < t_{1i}^0(T_{Di}^0) < t_{2i}^0(T_{Di}^0) < T_{Di}^0, \quad (6.2)$$

$$t_{1i}^0 < T_C, \quad (6.3)$$

where t_{1i}^0 , t_{2i}^0 and T_{Di}^0 are functions of T_C . One choice satisfying this condition is

$$T_C(p_C^0) = \frac{X_C}{v_C(p_C^0)} \times 0.999. \quad (6.4)$$

Using Eqs. (6.4) and (6.1), the oscillation probabilities are calculated numerically.

The oscillation probabilities with an infinite lifetime and a finite lifetime are shown in Figs.2 and 3, respectively. In Figs. 2 and 3, the oscillation length becomes longer than that of the standard formula when the wave packet sizes are smaller than 3.0×10^{-15} m, and the amplitude of the oscillation probability becomes smaller than 1 as X_B becomes larger or as the wave packet sizes become smaller.

In Figs. 4 (a), (b), (c) and (d), we compare the oscillation probabilities of the infinite lifetime with those of the finite lifetime at $\sigma_x = 2.0 \times 10^{-15}$ m for (a) and (b) and $\sigma_x = 1.0 \times 10^{-15}$ m for (c) and (d). From Fig. 4, it is seen that the oscillation length is longer and the amplitude of oscillation is smaller when the lifetime is infinite.

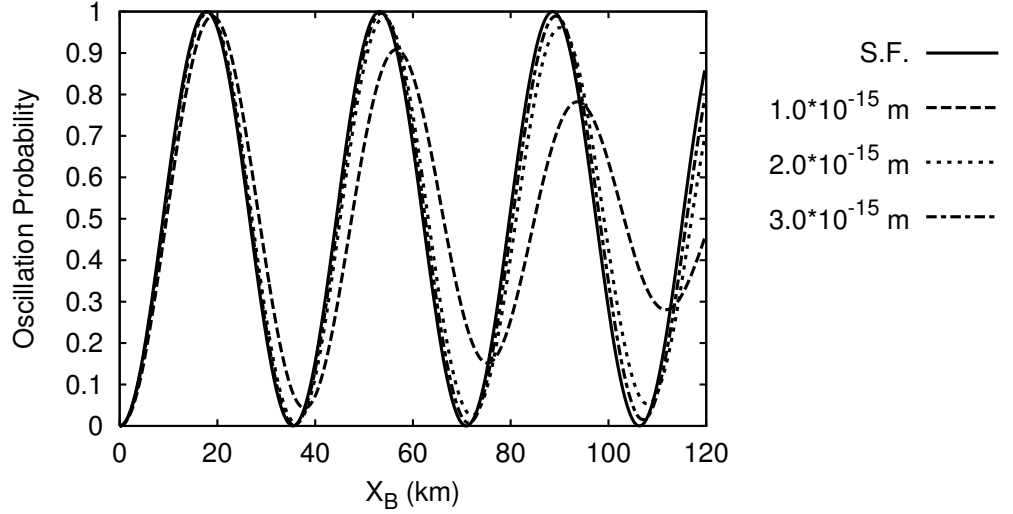


Fig. 2. The DIF oscillation probability with infinite lifetime. The solid curve represents the standard formula (S.F.), and the dashed, dotted and dashed-dotted curves correspond to the cases in which the wave packet sizes are 1.0×10^{-15} m, 2.0×10^{-15} m and 3.0×10^{-15} m, respectively. The horizontal axis is the position of B , X_B (km).

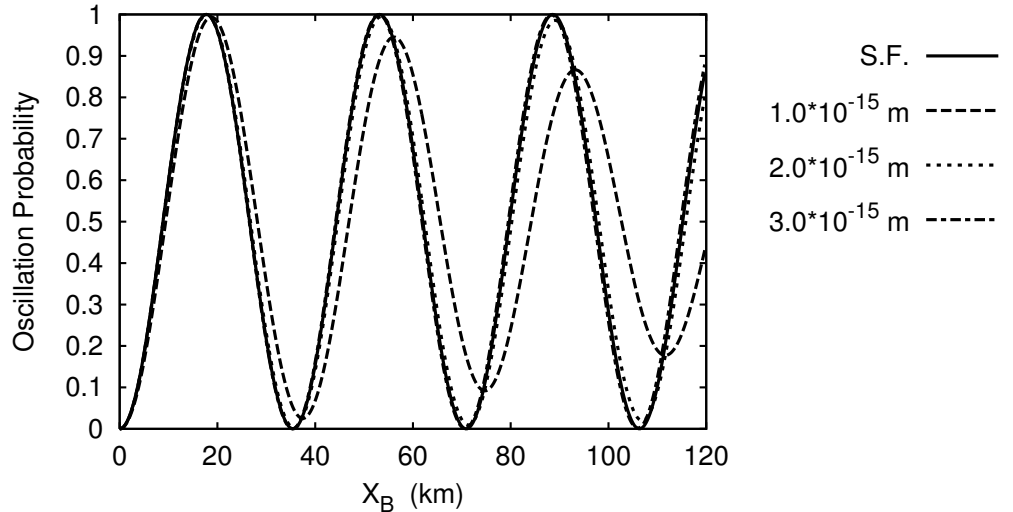


Fig. 3. The DIF oscillation probability with finite lifetime. The solid curve represents the standard formula (S.F.), and the dashed, dotted and dashed-dotted curves correspond to the cases the wave packet sizes are 1.0×10^{-15} m, 2.0×10^{-15} m and 3.0×10^{-15} m, respectively. The horizontal axis is the position of B , X_B (km).

The increase of oscillation length is caused by the increase of the time widths, $\bar{\sigma}_{t_{1i}}$ and $\bar{\sigma}_{T_i}$, in the coefficients in Eq. (3-11). In the following, we clarify the reason that the oscillation length increases with the time widths.

In Fig. 5, the p_C^0 dependences of the time widths are shown. From Figs. 5 (a) and (b), it is seen that $\bar{\sigma}_{t_{1i}}$ and $\bar{\sigma}_{T_i}$ grow with p_C^0 . From Eq. (2-18), it is seen that H loses its t_1

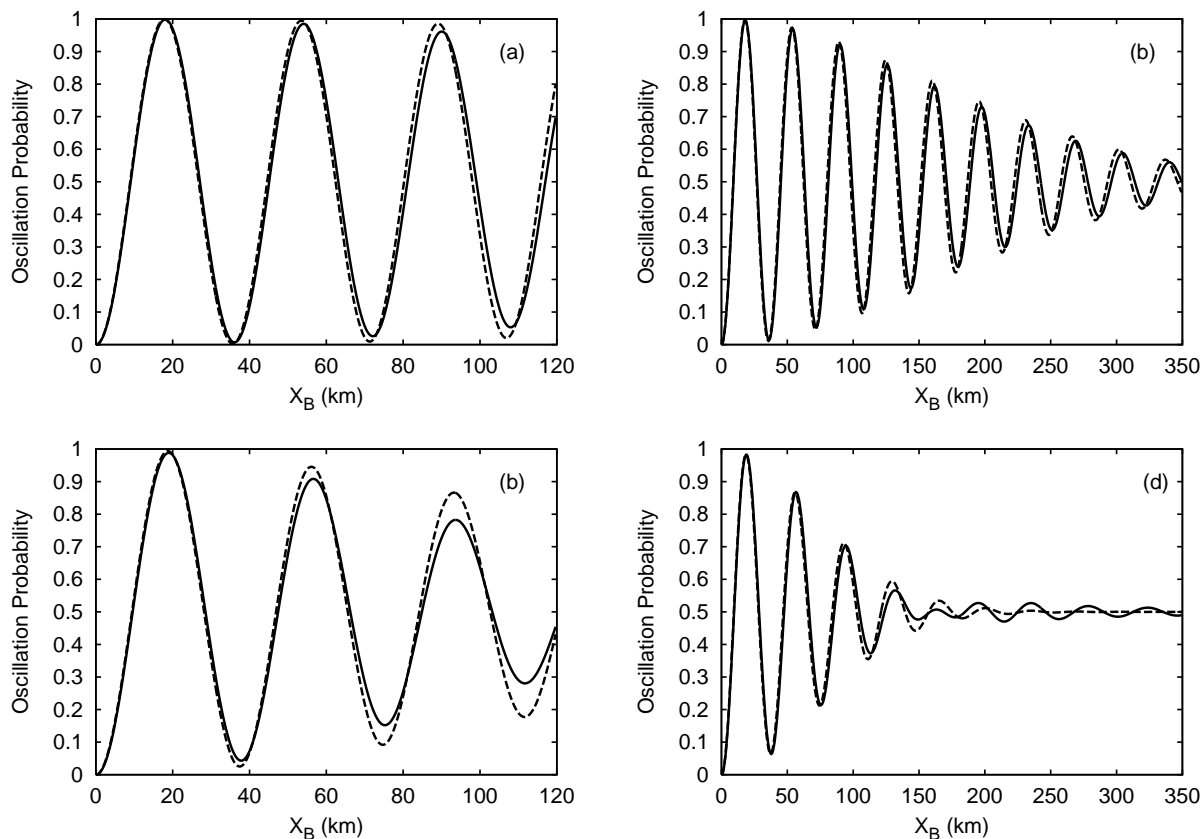


Fig. 4. The oscillation probabilities at $\sigma_x = 2.0 \times 10^{-15}$ m in (a) and (b), and those at $\sigma_x = 1.0 \times 10^{-15}$ m in (c) and (d). The solid curves represent the oscillation probabilities with infinite lifetime and the dashed curves represent those with finite lifetime.

dependence when v_C equals v_A . As we mentioned in the last part of Section 4, this growth of the time widths shifts the peak of the oscillation probability upward from that of the Gaussian in Eq. (3-11).

Figure 6 (a) shows the Gaussian function $\exp(2A_i)$ in the infinite lifetime case, and Fig. 6 (b) shows the absolute square of total amplitude Eq. (3-11), in which the maximum values are normalized to unity, at $\sigma = 1.0, 2.0, 3.0, 4.0 \times 10^{-15}$ m, respectively. From Fig. 6 (a), it is seen that the peaks of the Gaussian function are independent of the wave packet sizes. From Fig. (6) (b), it is seen that the peaks of the oscillation probability depend on the wave packet sizes. For large $\sigma_x (> 4.0 \times 10^{-15}$ m), the peaks of the oscillation probability are the same. But for small $\sigma_x (< 4.0 \times 10^{-15}$ m), the peaks of the oscillation probability are different from those of the Gaussian functions. This happens because the time widths grow with p_C^0 in Fig. 5 and the width of the Gaussian function becomes large in Fig. 6 (a). Then, the main contribution to the oscillation phase, Eq. (3-9) in Eq. (6-1), comes from the higher

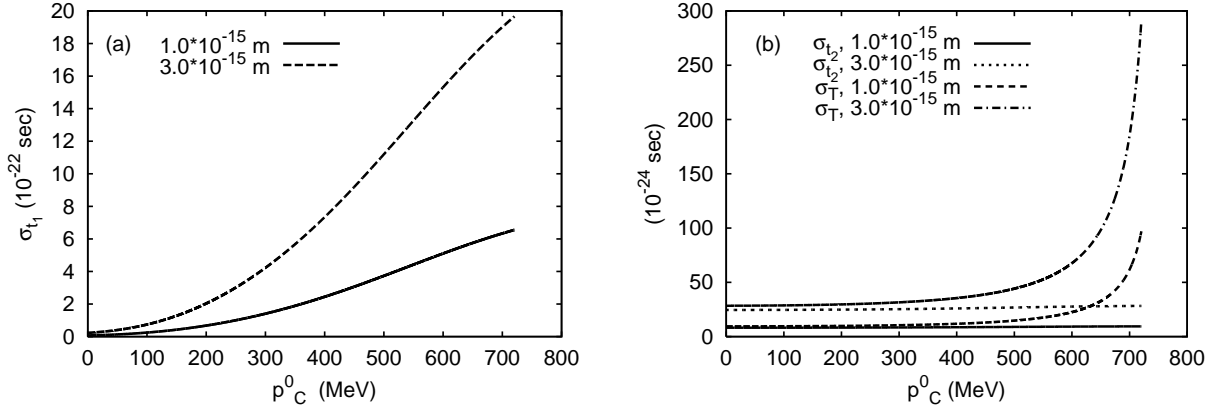


Fig. 5. (a): The p_C^0 dependence of $\bar{\sigma}_{t_1}$. The solid curve corresponds to $\bar{\sigma}_{t_1}$ at $\sigma_x = 1.0 \times 10^{-15}$ m, and the dashed curve corresponds to $\sigma_x = 3.0 \times 10^{-15}$ m. (b) :The p_C^0 dependence of $\bar{\sigma}_{t_2}$ and $\bar{\sigma}_T$. The solid and dotted curves represent $\bar{\sigma}_{t_2}$ at $\sigma_x = 1.0 \times 10^{-15}$ m and $\sigma_x = 3.0 \times 10^{-15}$ m, and the dashed and dashed-dotted curves are $\bar{\sigma}_T$ at $\sigma_x = 1.0 \times 10^{-15}$ m and $\sigma_x = 3.0 \times 10^{-15}$ m.

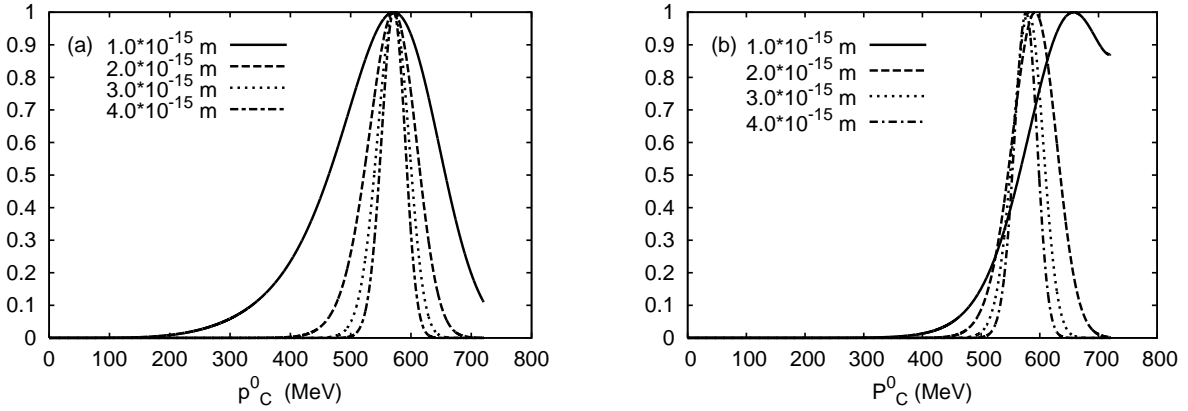


Fig. 6. (a): The p_C^0 dependence of the Gaussian function. (b): The p_C^0 dependence of the first term in Eq. (3.11). The solid curve represents $\sigma = 1.0 \times 10^{-15}$ m, and the dashed, dotted and dashed-dotted curves represent 2.0×10^{-15} , 3.0×10^{-15} and 4.0×10^{-15} m, respectively, in both graphs.

p_C^0 region.

Figure 7 displays the p_C^0 dependence of the ratio of the phase difference Eq. (3.9) to that of the standard formula for $X_B = 20, 60$ and 90 km :

$$\text{Phase Ratio} = \Theta_{21}(\tilde{T}_D^0) / \left(\frac{\Delta m_{21}^2 X_B}{2E} \right). \quad (6.5)$$

Here X_B is regarded as being the same as the travel distance of intermediate particles, and the energy E in the phase of the standard formula is determined by $\Delta P = 0$ and

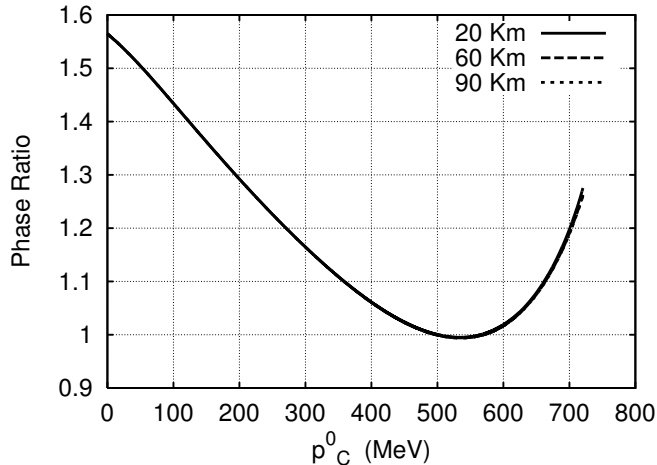


Fig. 7. The p_C^0 dependence of the ratio of oscillation phases. The solid, dashed and dotted curves represent the ratios at $X_B = 20, 60, 90$ km, respectively.

$\Delta\tilde{E}_1^0 \simeq \Delta\tilde{E}_2^0 \simeq 0$. From Fig. 7, it is seen that the ratio is almost independent of X_B but depends on p_C^0 . As is shown in Eq. (3·19), the phase ratio should become 1 at the solution $\Delta P = 0$ and $\Delta\tilde{E}_1^0 = \Delta\tilde{E}_2^0 = 0$, $p_C^0 = 570$ MeV. When σ_x is larger than 3.0×10^{-15} m, the main contribution to the integral in Eq. (6·1) comes from the region where the energy and momentum are conserved. Equation (6·1) is almost the same as the standard formula. But from Fig. 6, when σ_x is smaller than 3.0×10^{-15} m, the peak of the Gaussian part in the integrand moves to higher p_C^0 region than that of Fig. 6 (a), and the main contribution to Eq. (6·1) comes from the higher p_C^0 region. Then, the oscillation length becomes longer than that of the standard formula.

In the case that the particle A has a finite lifetime, the main contribution to the integral comes from the lower p_C^0 region, because of the presence of the lifetime in Eq. (4·7).

Figure 8 (a) displays the p_C^0 dependence of $\exp(-\Gamma t_{1_i}^0)$, and (b) displays the p_C^0 dependence of the absolute square of the amplitude (4·6), in which the maximum values are normalized to unity, at $\sigma = 1.0, 2.0, 3.0, 4.0 \times 10^{-15}$ m. The quantity $\exp(-\Gamma t_{1_i}^0)$ is almost independent of X_B and σ_x . From Fig. 8 (b), the peaks of the oscillation probability Eq. (4·6) shift to the lower p_C^0 region as the wave packet sizes become small.

The phase ratio Eq. (6·5) with finite lifetime is almost the same as that with infinite lifetime, because the lifetime τ is much larger than the time widths. Therefore, from Fig. 7, the oscillation length is longer than that of the standard formula when the wave packet sizes are smaller than 2.0×10^{-15} m and are slightly smaller than that of the standard formula when σ_x is larger than 3.0×10^{-15} m.

Figure 9 displays the p_C^0 dependence of the absolute square of the flavor changing amplitudes around $X_B = 37$ km. It is seen that the peaks of the absolute square of the amplitudes

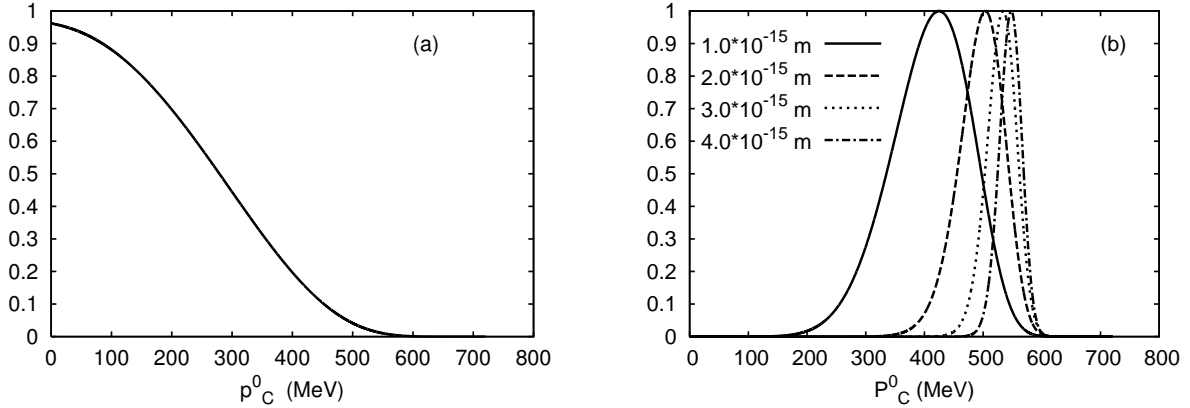


Fig. 8. (a): $\exp(-\Gamma t_{1i}^0)$ in the exponent of Eq. (4.6). (b): The first term in Eq. (4.6). The solid and dashed curves correspond to 1.0×10^{-15} m and 2.0×10^{-15} m, and the dotted and dashed-dotted curves correspond to 3.0×10^{-15} m and 4.0×10^{-15} m, respectively.

change and the shape of each amplitude is deformed with distance. The Gaussian shapes

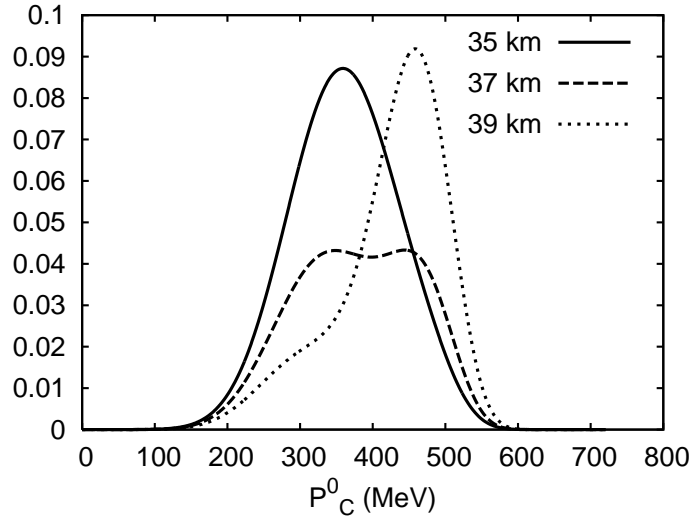


Fig. 9. p_C^0 dependence of the absolute square of the flavor changing amplitude at $\sigma_x = 1.0 \times 10^{-15}$ m. The vertical axis is normalized by the value of $|S|^2$ at $X_B = 18$ km. The solid curve represents the flavor conserving process at $X_B = 35$ km, and the dashed and dotted curves represent the flavor changing processes at $X_B = 37, 39$ km.

of the amplitudes are deformed by the cosine in the oscillation term. The behavior of the oscillation depends on X_B as well as p_C^0 , since the phase is proportional to $X_B/|\mathbf{k}^0|$. Then, as a result, the change and deformation given in Fig. 9 occur. This effect is seen clearly around the oscillation minimum.

6.2. Case 2 : Decay at rest

In the DAR, the intermediate particles I and particle C are produced by the decay of particle A at rest. The particle I is scattered by the particle B at rest, and then the particle D appears.

For the same reason as in case 1, X_C is set to -5.0 m and T_C is given as

$$T_C(p_C^0) = \frac{X_C}{v_C(p_C^0)} \times 2.0. \quad (6.6)$$

Because the source particle A is at rest, the numerical factor in $T_C(p_C^0)$ must be greater than 1 to satisfy the conditions (6.2) and (6.3). Here we take this factor to be 2.

The oscillation probabilities with finite lifetime are shown in Fig. 10. It is seen again that

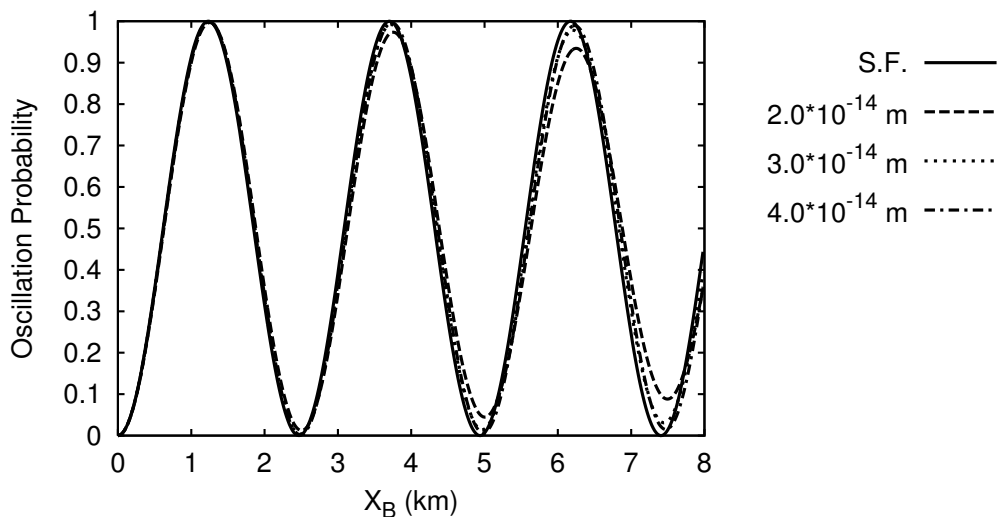


Fig. 10. The DAR oscillation probability with infinite lifetime: The solid curve represents the standard formula (S.F.), and the dashed, dotted and dashed-dotted curves correspond to the cases in which the wave packet sizes are 2.0×10^{-14} m, 3.0×10^{-14} m and 4.0×10^{-14} m, respectively. The horizontal axis is the position of B , X_B (km).

the amplitude of the oscillation becomes smaller and the period of the oscillation probability becomes longer than that of the standard formula as the wave packet sizes become smaller than 4.0×10^{-14} m.

In this case, t_{1i}^0 is almost zero, since the particle A is at rest. Because of this, there are no significant differences between the source particle with a finite lifetime and an infinite lifetime.

6.3. Case 3 : Low energy

In the last case, the intermediate particles are produced by the decay of the heavy particle A in flight. The central value of its momentum is about 1.3 MeV, which is much lower than

in case 1. The particles A and C have larger masses and smaller momenta than in the other two cases.

In contrast to the above two cases, this case corresponds to the solar neutrinos from ${}^7\text{Be}$ decays. The change of quantum mechanical states by scatterings is considered to be equivalent to detection or observation. Therefore the detection time of C is taken to the relaxation time, which is assumed to be the same value of particle A , and X_C is given as a function of p_C^0 . The quantities T_C and X_C are

$$T_C = \tau, \quad (6.7)$$

$$X_C(p_C^0) = 1.5 \times T_C v_C(p_C^0), \quad (6.8)$$

where τ is the relaxation time of the particle A , and its value is set to 10^{-12} sec.

In Fig. 11, the oscillation probability with finite lifetime is shown. In this case, the

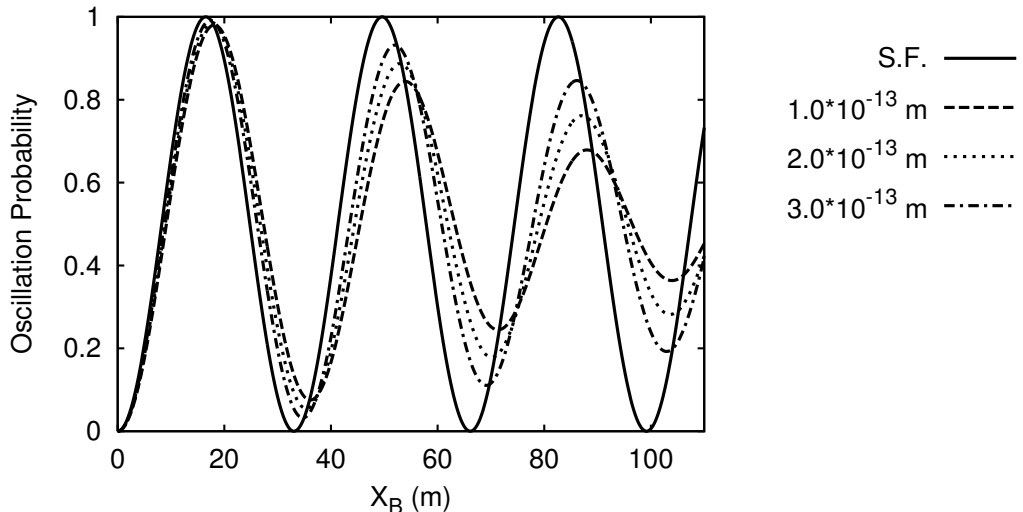


Fig. 11. The LOW oscillation probability with lifetime: The solid curve represents the standard formula (S.F.), and the dashed, dotted and dashed-dotted curves correspond to the case in which the wave packet sizes are 1.0×10^{-13} m, 2.0×10^{-13} m and 3.0×10^{-13} m, respectively. The horizontal axis is the position of B , X_B (m).

oscillation length becomes longer and the oscillation amplitude becomes smaller again. The wave packet effect becomes observable if the wave packet sizes are of order 10^{-13} m. A wave packet size of order 10^{-13} m is larger than those for the DIF and DAR cases. This is because the central values of the momenta are lower than in the DIF and DAR cases.

§7. Discussion and conclusion

In this paper, we have studied particle oscillations in the intermediate state of transition amplitudes of wave packets based on a simple scalar model. A source particle, a target

particle, and two scattered particles are the wave packets. In this situation, wave functions do not spread infinitely, but are localized within a finite width σ_x , and interference occurs only among intermediate particles that overlap spatially. This interference disappears and the oscillation probability deviates from those of the standard formula in parameter regions where the intermediate particles are separated spatially.

We computed the total oscillation probability and the phase factor of the amplitude numerically. We found that the oscillation probability agrees with that of the standard formula if the wave packet sizes are of semi-macroscopic values, and that the oscillation probability deviates from those of the standard formula in extreme parameter regions. This occurs when the wave packet sizes are of the order of 10^{-13} m or smaller. In this region, the wave packet size effects become visible. The oscillation amplitude becomes smaller and the oscillation period becomes larger than those of the standard formula. We hope that this region may be realized experimentally and that the modified formula found here will be tested in the future.

Although our results were obtained on the basis of a simple scalar model, we hope that for precision measurements of the neutrino parameters such as masses, the MNS matrix, and others, our considerations will be valuable.

Acknowledgements

This work was partially supported by a special Grant-in-Aid for the Promotion of Education and Science from Hokkaido University and a Grant-in-Aid for Scientific Research on Priority Areas (Dynamics of Superstrings and Field Theories, Grant No.13135201), and a Grand-in-Aid for Scientific Research on Priority Areas (Progress in Elementary Particle Physics of the 21st Century through Discoveries of Higgs Boson and Supersymmetry, Grand No. 16081201), provided by the Ministry of Education, Culture, Sports, Science and Technology, Japan, and the Nukazawa Science Foundation.

Appendix A

— The Center Times and the Time Widths —

In this appendix, we give the explicit forms of the time widths ($\bar{\sigma}_{t_{1i}}^2, \bar{\sigma}_{t_{2i}}^2, \bar{\sigma}_{T_{Di}}^2$) and the center times ($t_{1i}^0, t_{2i}^0, T_{Di}^0$). We omit the mass index i for simplicity. However, we note that one can easily obtain the center times and the time widths for specific mass eigenstates by replacing ν_I with ν_i .

The time widths and the center times are written in terms of the time derivatives of the

classical trajectory. The classical trajectory given in Eq. (2·15) is

$$Z_i(t_1, t_2, T_D) = \frac{\sigma_{AC}^2 \sigma_{BD}^2}{\sigma^2} \mathbf{F}_i^2(t_1, t_2, T_D) + \frac{\sigma_B^2 \sigma_D^2}{\sigma_{BD}^2} \mathbf{G}^2(t_2, T_D) + \frac{\sigma_A^2 \sigma_C^2}{\sigma_{AC}^2} \mathbf{H}^2(t_1), \quad (\text{A}\cdot 1)$$

$$\mathbf{F}_i(t_1, t_2, T_D) = \mathbf{x}_2^0(t_2, T_D) - \mathbf{x}_1^0(t_1) - \mathbf{v}_i(t_2 - t_1), \quad (\text{A}\cdot 2)$$

$$\mathbf{G}(t_2, T_D) = \mathbf{X}_D - \mathbf{X}_B - t_2 \mathbf{v}_B - (T_D - t_2) \mathbf{v}_D, \quad (\text{A}\cdot 3)$$

$$\mathbf{H}(t_1) = \mathbf{X}_C - \mathbf{X}_A - t_1 \mathbf{v}_A - (T_C - t_1) \mathbf{v}_C. \quad (\text{A}\cdot 4)$$

We use following abbreviated expressions for the time derivatives of the classical trajectory :

$$Z_{11} \equiv \frac{\partial^2 Z(t_1, t_2, T_D)}{\partial^2 t_1} = 2 \frac{\sigma_{AC}^2 \sigma_{BD}^2}{\sigma^2} \mathbf{F}_1^2 + 2 \frac{\sigma_A^2 \sigma_C^2}{\sigma_{AC}^2} \mathbf{H}_1^2, \quad (\text{A}\cdot 5)$$

$$Z_{22} \equiv \frac{\partial^2 Z(t_1, t_2, T_D)}{\partial^2 t_2} = 2 \frac{\sigma_{AC}^2 \sigma_{BD}^2}{\sigma^2} \mathbf{F}_2^2 + 2 \frac{\sigma_B^2 \sigma_D^2}{\sigma_{BD}^2} \mathbf{G}_2^2, \quad (\text{A}\cdot 6)$$

$$Z_{TT} \equiv \frac{\partial^2 Z(t_1, t_2, T_D)}{\partial^2 T_D} = 2 \frac{\sigma_{AC}^2 \sigma_{BD}^2}{\sigma^2} \mathbf{F}_T^2 + 2 \frac{\sigma_B^2 \sigma_D^2}{\sigma_{BD}^2} \mathbf{G}_T^2, \quad (\text{A}\cdot 7)$$

$$Z_{12} \equiv \frac{\partial^2 Z(t_1, t_2, T_D)}{\partial t_1 \partial t_2} = 2 \frac{\sigma_{AC}^2 \sigma_{BD}^2}{\sigma^2} \mathbf{F}_1 \cdot \mathbf{F}_2, \quad (\text{A}\cdot 8)$$

$$Z_{1T} \equiv \frac{\partial^2 Z(t_1, t_2, T_D)}{\partial t_1 \partial T_D} = 2 \frac{\sigma_{AC}^2 \sigma_{BD}^2}{\sigma^2} \mathbf{F}_1 \cdot \mathbf{F}_T, \quad (\text{A}\cdot 9)$$

$$Z_{2T} \equiv \frac{\partial^2 Z(t_1, t_2, T_D)}{\partial t_2 \partial T_D} = 2 \frac{\sigma_{AC}^2 \sigma_{BD}^2}{\sigma^2} \mathbf{F}_2 \cdot \mathbf{F}_T + 2 \frac{\sigma_B^2 \sigma_D^2}{\sigma_{BD}^2} \mathbf{G}_2 \cdot \mathbf{G}_T, \quad (\text{A}\cdot 10)$$

and

$$Z_{10} \equiv \left. \frac{\partial Z(t_1, t_2, T_D)}{\partial t_1} \right|_{\substack{t_1=0 \\ t_2=0}} = 2 \frac{\sigma_{AC}^2 \sigma_{BD}^2}{\sigma^2} \mathbf{F}_1 \cdot (\mathbf{F}_0 + \mathbf{F}_T T_D) + 2 \frac{\sigma_A^2 \sigma_C^2}{\sigma_{AC}^2} \mathbf{H}_1 \cdot \mathbf{H}_0, \quad (\text{A}\cdot 11)$$

$$Z_{20} \equiv \left. \frac{\partial Z(t_1, t_2, T_D)}{\partial t_2} \right|_{\substack{t_1=0 \\ t_2=0}} = 2 \frac{\sigma_{AC}^2 \sigma_{BD}^2}{\sigma^2} \mathbf{F}_2 \cdot (\mathbf{F}_0 + \mathbf{F}_T T_D) + 2 \frac{\sigma_B^2 \sigma_D^2}{\sigma_{BD}^2} \mathbf{G}_2 \cdot (\mathbf{G}_0 + \mathbf{G}_T T_D), \quad (\text{A}\cdot 12)$$

$$\begin{aligned} Z_{T0} \equiv \left. \frac{\partial Z(t_1, t_2, T_D)}{\partial T_D} \right|_{\substack{t_1=t_1^0(0) \\ t_2=t_2^0(0) \\ T_D=0}} &= 2 \frac{\sigma_{AC}^2 \sigma_{BD}^2}{\sigma^2} \mathbf{F}_T \cdot (\mathbf{F}_0 + \mathbf{F}_1 t_1^0(0) + \mathbf{F}_2 t_2^0(0)) \\ &\quad + 2 \frac{\sigma_B^2 \sigma_D^2}{\sigma_{BD}^2} \mathbf{G}_T \cdot (\mathbf{G}_0 + \mathbf{G}_2 t_2^0(0)). \end{aligned} \quad (\text{A}\cdot 13)$$

Here, \mathbf{F}_i , \mathbf{G}_i and \mathbf{H}_i ($i = 0, 1, 2, T$) are the coefficient vectors of t_1 , t_2 and T , and are given as

$$\mathbf{F}_0 = \frac{\sigma_B^2 \mathbf{X}_B + \sigma_D^2 \mathbf{X}_D}{\sigma_{BD}^2} - \frac{\sigma_A^2 \mathbf{X}_A + \sigma_C^2 (\mathbf{X}_C - T_C \mathbf{v}_C)}{\sigma_{AC}^2}, \quad (\text{A}\cdot 14)$$

$$\mathbf{F}_1 = -\frac{\sigma_A^2 \mathbf{v}_A + \sigma_C^2 \mathbf{v}_C}{\sigma_{AC}^2} + \mathbf{v}_I, \quad \mathbf{F}_2 = \frac{\sigma_B^2 \mathbf{v}_B + \sigma_D^2 \mathbf{v}_D}{\sigma_{BD}^2} - \mathbf{v}_I, \quad \mathbf{F}_T = -\frac{\sigma_D^2 \mathbf{v}_D}{\sigma_{BD}^2}, \quad (\text{A}\cdot\text{15})$$

$$\mathbf{G}_0 = \mathbf{X}_D - \mathbf{X}_B, \quad \mathbf{G}_2 = -\mathbf{v}_B + \mathbf{v}_D, \quad \mathbf{G}_T = -\mathbf{v}_D, \quad (\text{A}\cdot\text{16})$$

$$\mathbf{H}_0 = \mathbf{X}_C - \mathbf{X}_A - T_C \mathbf{v}_C, \quad \mathbf{H}_1 = -\mathbf{v}_A + \mathbf{v}_C. \quad (\text{A}\cdot\text{17})$$

Using these functions, the time widths and the center times are written as follows :

$$\frac{1}{\bar{\sigma}_{t_1}^2} = \frac{1}{2} Z_{11}, \quad (\text{A}\cdot\text{18})$$

$$\frac{1}{\bar{\sigma}_{t_2}^2} = \frac{1}{2} Z_{22} - \frac{1}{4} \bar{\sigma}_{t_1}^2 Z_{12}^2, \quad (\text{A}\cdot\text{19})$$

$$\Delta t_1^0 = -\frac{1}{2} \bar{\sigma}_{t_1}^2 \bar{\sigma}_{t_2} Z_{12}, \quad (\text{A}\cdot\text{20})$$

$$\frac{1}{\bar{\sigma}_T^2} = \frac{1}{2} Z_{TT} - \frac{1}{4} (\bar{\sigma}_{t_1}^2 + \Delta t_1^0) Z_{1T}^2 - \frac{1}{2} \bar{\sigma}_{t_2} \Delta t_1^0 Z_{1T} Z_{2T} - \frac{1}{4} \bar{\sigma}_{t_2}^2 Z_{2T}^2, \quad (\text{A}\cdot\text{21})$$

and

$$t_1^0(T_D) = -\frac{1}{2} (\bar{\sigma}_{t_1}^2 + \Delta t_1^0) Z_{10} - \frac{1}{2} \bar{\sigma}_{t_2} \Delta t_1^0 Z_{20}, \quad (\text{A}\cdot\text{22})$$

$$t_2^0(T_D) = -\frac{1}{2} \bar{\sigma}_{t_2} \Delta t_1^0 Z_{10} - \frac{1}{2} \bar{\sigma}_{t_2}^2 Z_{20}, \quad (\text{A}\cdot\text{23})$$

$$T_D^0 = -\frac{1}{2} \bar{\sigma}_T^2 Z_{T0}. \quad (\text{A}\cdot\text{24})$$

Appendix B

— Measurement of Transition Probability —

Following the standard interpretation of measurement in quantum mechanics, the square of the absolute value of the amplitude, $|S|^2$, gives the transition probability from the initial state (2.7), which is prepared at $t = 0$, to the final state Eq. (2.8), which is defined at $t = T_D$. For the probability interpretation to make sense, each observation at the final state should be made independently and exclusively. This is, when one value is observed for an observation, the other value should not be observed. The state of one value is different from the state of a different value. Conversely, the final state should be different if the corresponding values are different.

Because the orthogonality of states described by the wave packet is peculiar, the total probability should be defined in a manner that is consistent with experiments. This problem has been solved in usual scatterings, where the wave packet effects are negligibly small. The detector used in experiments has a finite macroscopic size, and the total rate observed in a macroscopic detector is computed with a continuous momentum. The total observed probability is obtained by integrating the square of the absolute value of the amplitude with

a continuous momentum. Therefore this problem has been solved in the case of normal scattering.

In neutrino scattering, the energy scale is very small, and the event rate is also very small. Events occur so infrequently that the detector is in different quantum states that are orthogonal to each other. Also, the detector has a macroscopic size. Consequently, the total rate observed in a macroscopic detector within a finite detection time is computed by integrating the probability with the central value of the momentum and the time.

References

- 1) T. Yabuki and K. Ishikawa, *Prog. Theor. Phys.* **108** (2002), 347.
- 2) Marvin L. Goldberger and Kenneth M. Watson, "COLLISION THEORY", JOHN WILEY & SONS, Inc. New York-London-Sydney, (1965)
- 3) B. Kayser, *Phys. Rev. D* **24** (1981), 110; *Nucl. Phys.* **B19**(Proc.Suppl) (1991), 177.
- 4) J. Rich, D. lioyd. Owen, M. Spirio, *Phys. Rep.* **151** (1987), 267.
J. Rich, *Phys. Rev. D* **48** (1993), 4318.
- 5) M. Fukugida and T. Yanagida, in "Physics and Astrophysics of Neutrinos" edited by M. Fukugida and A. Suzuki, Springer-Verlag(Tokyo), 1-213(1999).
- 6) C. Giunti, C. W. Kim, and U. W. Lee, *Phys. Rev. D* **44** (1991), 3635.
See also references in, C. Giunti, C. W. Kim, and U. W. Lee, *Phys. Lett. B* **421** (1998), 237. C. Giunti, C. W. Kim, hep-ph/0011074 (2000).
- 7) W. Grimus, P. Stockinger and S. Mohanty, *Phys. Rev. D* **54** (1996), 3414.
See also references in, W. Grimus, P. Stockinger and S. Mohanty, *Phys. Rev. D* **57** (1998), 1920, hep-ph/9909341(1999).
- 8) M. Nauenberg, *Phys. Lett. B* **447** (1999), 23.
- 9) Z. Maki, M. Nakagawa and S. Sakata, *Prog. Theor. Phys.* **28** (1962), 870.
- 10) B. Pontecorvo, *Zh. Eksp. Teor. Fiz.* **53** (1967), 1717; *Sov. Phys. JETP* **26** (1968), 984.
- 11) K. Kiers , N. Nussinov and N. Weisis, *Phys. Rev. D* **53** (1996), 537.
- 12) S. Nussinov, *Phys. Lett. B* **63** (1976), 201.
- 13) L. Krauss and F. Wilczek, *Phys. Rev. Lett.* **55** (1985), 122.
- 14) A. Loeb, *Phys. Rev. D* **39** (1989), 1009.